Fault-Tolerant Building Change Detection From Urban High-Resolution Remote Sensing Imagery

Yuqi Tang, Xin Huang, and Liangpei Zhang

Abstract—This letter proposes a novel change detection model, focusing on building change information extraction from urban high-resolution imagery. It consists of two blocks: 1) building interest-point detection, using the morphological building index (MBI) and the Harris detector; and 2) multitemporal building interest-point matching and the fault-tolerant change detection. The proposed method is insensitive to the geometrical differences of buildings caused by different imaging conditions in the multitemporal high-resolution imagery and is able to significantly reduce false alarms. Experiments showed that the proposed method was effective for building change detection from multitemporal urban high-resolution images. Moreover, the effectiveness of the algorithm was validated by comparing with the morphological change vector analysis (CVA), parcel-based CVA, and MBI-based CVA.

Index Terms—Building, fault tolerance, high resolution, morphological.

I. INTRODUCTION

NOWADAYS, urban sprawl is a worldwide challenge. It is necessary to detect the land-cover/use changes occurring with urban sprawl and make plans for sustainable development. Change detection is one of the main applications of remote sensing as multitemporal satellite data are an effective data source for identifying where changes take place [1], [2]. With the development of spatial imaging techniques, the remote sensing imagery acquired by high-spatial-resolution satellites has been widely used in change detection. However, it poses challenges to the traditional spectral-based change detection techniques that are inadequate for representing spatial information of changed areas. To this aim, some studies have been reported on the exploitation of spatial approaches for change detection. Bovolo [3] incorporated object-based image analysis into change vector analysis (CVA) [4], by which the spatial features are combined with the spectral information for multitemporal image analysis. Pacifici and Del Frate [5] applied pulse-coupled neural networks to urban change detection. Gueguen *et al.* [6] proposed a change indicator by combining the local mutual and variation information between multitemporal images. Dalla

Mura *et al.* [7] proposed to jointly use morphological filtering and the CVA algorithm for high-resolution image change detection in order to filter out commission errors caused by the geometrical differences in the multitemporal images. Bovolo *et al.* [8] and Marchesi *et al.* [9] developed a polar framework for change detection to deal with the effects of residual misregistration and alleviate the misregistration errors.

Buildings are one of the most important targets for high-resolution urban monitoring [10], [11]; therefore, building detection has received increasing attention in recent years [12]. However, few studies have been reported concerning building change detection from high-resolution imagery. The challenges of this problem include the geometrical difference of buildings caused by the different view angles of sensors in multitemporal images, as well as the conditions of shadow resulting from different solar elevation angles.

In this letter, we propose to utilize geometrical properties, including the interest points and structural features of buildings, to identify the building change information in multitemporal images. In our method, building structures are automatically indicated using the morphological building index (MBI) [12], [13]. The interest points of buildings are then generated by the intersection of potential building pixels and the corner/edge pixels in the image. Subsequently, the corresponding buildings in the multitemporal images are matched using the building interest points. The proposed method aims to compare buildings and detect potential changes by a local building matching, rather than comparing the pixels or objects used in the traditional methods. This letter is organized as follows: Section II describes the proposed building change detection method. Experiments are reported in Section III. In Section IV, the proposed method is compared with several state-of-the-art change detection methods. Section V concludes this letter.

II. METHODOLOGY

The processing chain of the proposed methodology consists of two blocks: 1) detection of building interest points and 2) building interest-point matching and change detection.

A. Detection of Building Interest Points

The building interest points are detected by the following three steps.

Step 1—MBI: The MBI is able to automatically extract buildings from high-resolution imagery by characterizing the spectral–structural features of buildings with morphological operators [12], [13]. The spectral–structural characteristics of

buildings are represented by the differential morphological profiles (DMPs) of the top-hat by reconstruction with a series of linear structural elements (SEs). Calculation of the MBI is briefly introduced as follows, but a more comprehensive introduction to the MBI algorithm is given in [12].

The brightness image is first calculated by calculating the maximum value of multispectral bands for each pixel, i.e.,

$$B(x,y) = \max_{1 \le k \le K} (\text{band}_k(x,y)) \tag{1}$$

where $\text{band}_k(x,y)$ is the spectral value of pixel (x,y) at the kth band, and K is the number of multispectral bands. The DMPs of the white top-hat are defined based on the brightness image, i.e.,

$$\text{DMP}_{\text{W\_TH}}(d,s) = |\text{MP}_{\text{W\_TH}}(d, s+\Delta s) - \text{MP}_{\text{W\_TH}}(d,s)| \tag{2}$$

with

$$\begin{cases} \text{MP}_{\text{W\_TH}} = B - r_B^{\text{re}}(d,s), & \text{if } s > 0 \\ \text{MP}_{\text{W\_TH}} = B, & \text{if } s = 0 \end{cases}$$

where $r_B^{\text{re}}(d,s)$ denotes the opening-by-reconstruction of the brightness image B, and s and d indicate the scale and direction of a linear SE, respectively. Δs means the interval of the profile scales with $s_{\min} \le s \le s_{\max}$. MBI is defined as the average of the DMPs of the white top-hat profiles since buildings have large local contrast in different directions within the range of the chosen scales. Thus

$$\text{MBI} = \frac{\sum_{d,s} \text{DMP}_{\text{W\_TH}}(d,s)}{D \times S} \tag{3}$$

where D and S indicate the numbers of the direction and scale of the profiles, respectively. Since an increase in D does not result in higher accuracy for building extraction according to [12], the value of D is fixed at 4 in this letter. According to the spatial resolution of images and the characteristics of buildings, the sizes of SE (s_{max}, s_{min}, and Δs) are set to (2, 52, and 5).

Step 2—Harris Detector: The Harris detector was originally proposed for corner and edge detection from natural imagery [14], where a measure of the corner and edge response is constructed in order to select isolated corner pixels and thin edges. In this letter, it is employed to extract the interest points on building corners from the multitemporal images.

Step 3—Detection of Building Interest Points: The building interest points $I_b(x,y)$ are generated by integrating the interest points chosen by the Harris detector and the building structures extracted by the MBI algorithm, i.e.,

$$I_b(x,y) = \begin{cases} 0, & \text{MBI}(x,y) = 0 \text{ or } I(x,y) = 0 \\ 1, & \text{MBI}(x,y) > 0 \text{ and } I(x,y) = 1 \end{cases} \tag{4}$$

where $\text{MBI}(x,y)$ and $I(x,y)$ indicate the results of MBI building detection and Harris interest-point detection, respectively. This way, the interest points of potential building structures (i.e., $\text{MBI}(x,y) > 0$) are retained for the subsequent building matching in multitemporal images.
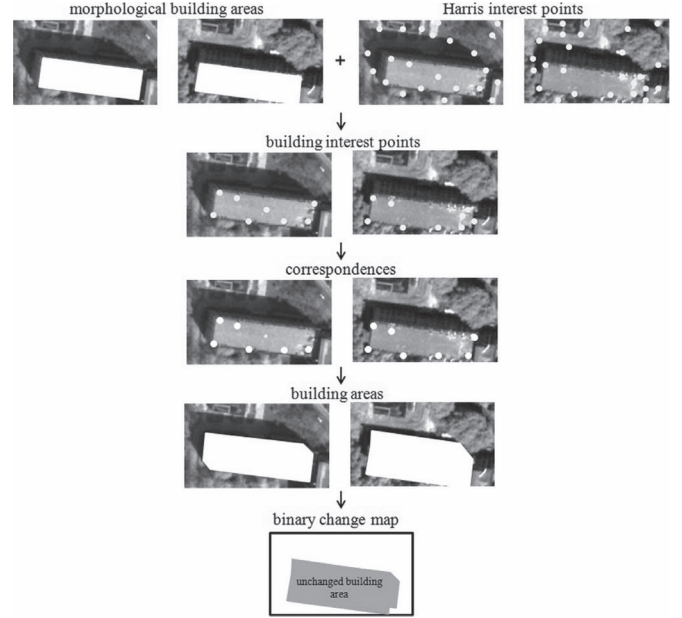

Fig. 1. Graphical example of the proposed method.

B. Building Change Detection Based on Interest-Point Matching

Step 1—Building Interest-Point Matching: Local image matching is a critical strategy for the proposed fault-tolerant change detection. A control network is constructed for each multitemporal image. The corresponding points are searched in a circle area according to the constraints of distance and angle compared with the starting point. The pair of points with the smallest differences in distance and angle is chosen as correspondences. If a building interest point does not have a correspondence in the other control network, it is regarded as an outlier. The correspondences stand for unchanged building structures, and the outliers are likely to be changed ones since they are not matched with any building point in the other image within the predefined range (e.g., distance and direction). It should be underlined that the image matching is similar to the method in [15], but differently, in this letter, we focus on the multitemporal matching of building interest points.

Step 2—Matching-Based Change Detection: After the correspondences of the building interest points are constructed in the multitemporal images, region growing is carried out separately in both images. This way, the neighboring building interest points are merged when their difference of MBI is less than a threshold T_{mbi}. The objects growing from outliers in either of the multitemporal images are regarded as changed buildings. Subsequently, an object-oriented fault-tolerant change detection algorithm is proposed to compare the corresponding building objects. The building change detection is carried out based on the following rule:

$$C(i)$$
$$= \begin{cases} 1, & \text{Obj}(i) \in \text{Obj}_1(i) \cup \text{Obj}_2(i) \\ & \text{and } |M_1(i) - M_2(i)| \ge T_{\text{spe}}, \quad i \in \{1, 2, \dots, N\} \\ 0, & \text{otherwise} \end{cases} \tag{5}$$
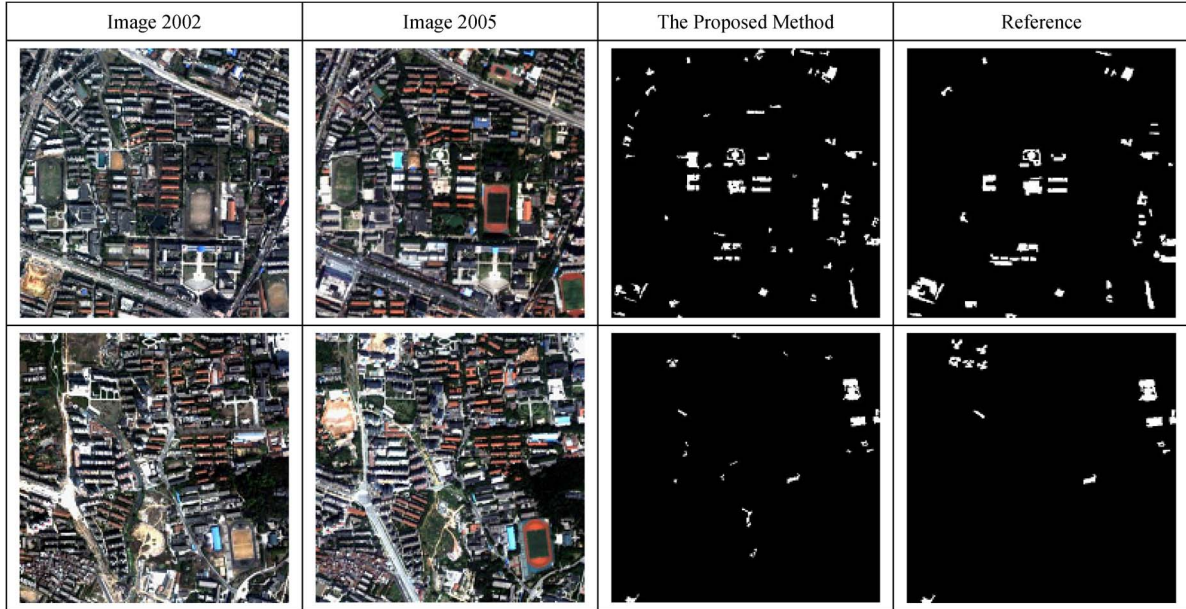
Fig. 2. Results of the proposed method for the multitemporal QuickBird Wuhan subsets. (The thresholds of T_{spe} are set to 5 and 18 for the two data sets, respectively.)

where $C(i)$ represents whether the object i is changed, with 0 and 1 for nonchange and change, respectively. $\mathrm{Obj}_1(i)$ and $\mathrm{Obj}_2(i)$ denote the ith pair of corresponding objects in the multitemporal images, and $M_1(i)$ and $M_2(i)$ are their spectral means, respectively. $\mathrm{Obj}(i)$ is the union of $\mathrm{Obj}_1(i)$ and $\mathrm{Obj}_2(i)$. N is the number of pairs of the corresponding building objects. If the difference of spectral means for the ith pair of corresponding building objects is larger than a user-defined threshold T_{spe}, the union area $\mathrm{Obj}(i)$ is regarded as changed. Otherwise, it is considered as unchanged. A graphical example of the proposed method is demonstrated in Fig. 1, from which it is shown that the proposed method can effectively tolerate the geometrical differences and suppress the false alarms for the building change detection.

III. EXPERIMENTS

The experiments are conducted on QuickBird images in 2002 and 2005 and on IKONOS images in 2002 and 2009. Both data sets are over typical urban areas of Wuhan, central China. In experiments, the preprocessing steps include coregistration and relative radiometric correction. The root mean square of registration is less than one pixel, and the radiometric correction is conducted by a linear regression. The reference of the building change information is manually delineated based on a field campaign in the experimental areas. Three indices are used to assess the results: correctness, completeness, and quality. Thus

$$\mathrm{Correctness} = \frac{\mathrm{TP}}{\mathrm{TP} + \mathrm{FP}} \qquad (6)$$

$$\mathrm{Completeness} = \frac{\mathrm{TP}}{\mathrm{TP} + \mathrm{FN}} \qquad (7)$$

$$\mathrm{Quality} = \frac{\mathrm{TP}}{\mathrm{TP} + \mathrm{FP} + \mathrm{FN}} \qquad (8)$$

where TP and FP are the numbers of changed pixels in the result, but changed and unchanged in the reference image, re-

TABLE I
PIXEL-BASED ACCURACY ASSESSMENT OF THE PROPOSED METHOD

Datasets	Correctness	Completeness	Quality
QuickBird 1	67.91%	69.64%	52.40%
QuickBird 2	81.75%	74.79%	64.09%
IKONOS	70.77%	62.23%	49.51%

TABLE II
OBJECT-ORIENTED ACCURACY ASSESSMENT
OF THE PROPOSED METHOD

Datasets	Correctness	Completeness	Quality
QuickBird 1	63.04%	82.86%	55.77%
QuickBird 2	81.82%	69.23%	60.00%
IKONOS	95.24%	71.43%	68.97%

spectively. FN is the number of changed pixels in the reference image, but detected as unchanged in the result.

A. QuickBird Data Set

The experimental results of QuickBird 2002 and 2005 data sets are shown in Fig. 2. The results obtained by the proposed method can be regarded as satisfactory compared with the reference map. Most of the changed buildings are detected in spite of some commission errors observed. There are also several omission errors in the bottom left of the image. Most of these errors can be partly attributed to the inaccuracy of the automatic building extraction based on MBI. However, it should be kept in mind that the whole processing chain is carried out without any training samples. Tables I and II (the first and second rows) show the pixel-based and object-oriented accuracy values of the proposed method, respectively.

B. IKONOS Data Set

This experiment refers to a Wuhan IKONOS data set, and the multitemporal images after the preprocessing are shown
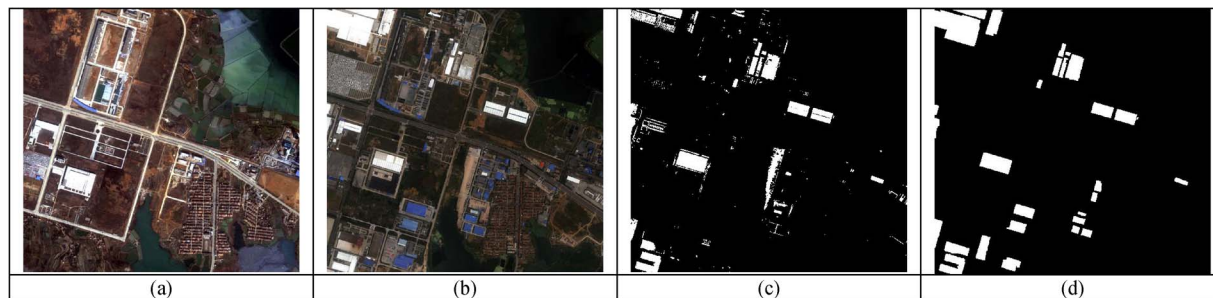
Fig. 3.   Result of the proposed method for the IKONOS data set. (a) 2002 image. (b) 2009 image. (c) Result of the proposed method. (d) Reference image. (The threshold of T_{spe} is set to 3.)
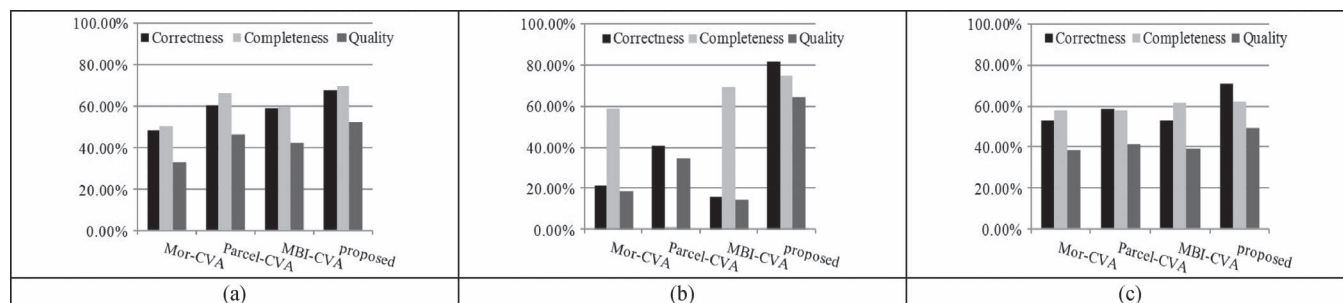

Fig. 4.   Quantitative comparison between different change detection methods for the (a) QuickBird 1 data set, (b) QuickBird 2 data set, and (c) IKONOS experiment.

in Fig. 3. The binary change map obtained by the proposed method and the reference image are shown in Fig. 3(c) and (d), respectively. Most of the changes are correctly detected in spite of a few commission and omission errors observed. The commission errors mainly result from the similar spectral attributes between buildings and other impervious areas such as roads and grounds. On the other hand, the omission errors refer to the building areas with relatively low brightness, which are difficult to extract by the MBI operator. Tables I and II (the third row) show the pixel-based and object-oriented quantitative accuracy values of the proposed method, respectively. Both quantitative indices and visual inspection show that the proposed method achieves satisfactory results, considering that the whole change detection is unsupervised, and without training and machine learning.

IV. COMPARATIVE STUDY

Here, the proposed method is compared with three state-of-the-art change detection methods.

1) Morphological CVA [7] (Mor-CVA): It is implemented by alternating the transformations of opening and closing by reconstruction with the result of the CVA with an increasing size of linear SE. According to the spatial resolutions of the data sets, the minimum and maximum lengths of linear SE in this letter are set to 2 and 12, respectively, with an increment of 2. This method is able to filter out commission errors caused by the pixel-based comparison and geometrical differences.

2) Parcel-based CVA [3] (Parcel-CVA): It is a recently developed object-oriented change detection method. The multitemporal parcel-based hierarchies of spatial context

are modeled by the fractal net evolution approach. The weights of the spectrum and compactness are 0.7 and 0.5, respectively. The scale is set to 10 according to the spatial resolution of the multitemporal images.

3) MBI-based CVA (MBI-CVA): It is a change detection algorithm focusing on buildings. The spectral bands are replaced by the multitemporal MBI feature images for the CVA. It can be viewed as an MBI-based prefiltering before the implementation of the CVA.

The accuracy indices of the three data sets are shown in Fig. 4(a)–(c), respectively, for the QuickBird 1, QuickBird 2, and IKONOS experiments. It is shown that, compared with other methods, the proposed fault-tolerant change detection algorithm achieves the highest correctness, completeness, and quality in all the three experiments. The proposed algorithm is able to significantly suppress false alarms since the multitemporal images are matched based on the building interest points. The change detection maps of the different algorithms are compared in Fig. 5. The visual comparison shows that the proposed algorithm achieves the most similar results with the reference. It is able to avoid the salt-and-pepper effects of the pixel-based change detection approaches. Moreover, the proposed algorithm is able to reduce the false alarms of the roads, which are spectrally similar to the buildings and hence lead to a number of commission errors (particularly in the IKONOS experiment).

V. CONCLUSION

In this letter, we have presented a building change detection method from urban high-resolution images, which is able to suppress the effect of geometrical differences caused by the
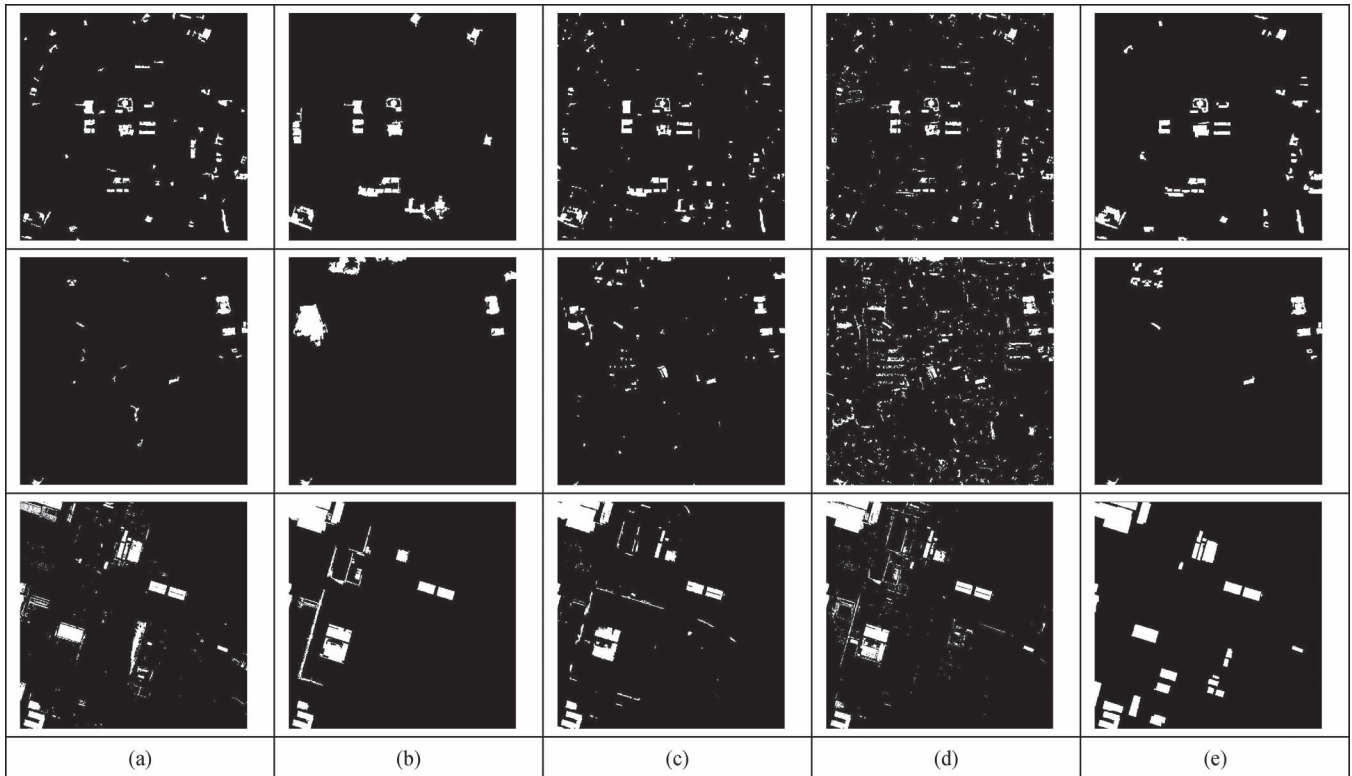
Fig. 5.　Qualitative comparisons of the binary change map of the (a) proposed method, (b) Mor-CVA, (c) Parcel-CVA, (d) MBI-CVA, and (e) reference image of the three data sets.

multitemporal high-resolution imaging conditions. In order to reduce these errors, a feature-matching approach was proposed in order to achieve the fault-tolerant change detection. The utilization of the MBI and the Harris detectors guarantee the effective extraction of building interest points. The interest-point matching within a range of distance and angle can effectively search for the correspondences of buildings in the multitemporal images. This way, the change detection between corresponding building objects is fault tolerant to the geometrical differences of buildings in multitemporal high-resolution images. The qualitative and quantitative analysis of the results obtained with three data sets validated the effectiveness of the proposed method. A comparison between the proposed method and several recently developed change detection methods revealed that the proposed method reduced the number of commission and omission errors significantly.

REFERENCES

[1] R. J. Radke, S. Andra, O. Al-Kofahi, and B. Roysam, "Image change detection algorithms: Systematic survey," *IEEE Trans. Image Process.*, vol. 14, no. 3, pp. 294–307, Aug. 2005.

[2] D. Lu, P. Mausel, E. Brondizio, and E. Moran, "Change detection techniques," *Int. J. Remote Sens.*, vol. 25, no. 12, pp. 2365–2407, Jun. 2004.

[3] F. Bovolo, "A multilevel parcel-based approach to change detection in very high resolution multitemporal images," *IEEE Geosci. Remote Sens. Lett.*, vol. 6, no. 1, pp. 33–37, Jan. 2009.

[4] R. D. Johnson and E. S. Kasischke, "Change vector analysis: A technique for the multispectral monitoring of land cover and condition," *Int. J. Remote Sens.*, vol. 19, no. 3, pp. 411–426, 1998.

[5] F. Pacifici and F. Del Frate, "Automatic change detection in very high resolution images with pulse-coupled neural networks," *IEEE Geosci. Remote Sens. Lett.*, vol. 7, no. 1, pp. 58–62, Jan. 2010.

[6] L. Gueguen, P. Soille, and M. Pesaresi, "Change detection based on information measure," *IEEE Trans. Geosci. Remote Sens.*, vol. 49, no. 11, pp. 4503–4515, Nov. 2011.

[7] M. Dalla Mura, "An unsupervised technique based on morphological filters for change detection in very high resolution images," *IEEE Geosci. Remote Sens. Lett.*, vol. 5, no. 3, pp. 433–437, Jul. 2008.

[8] F. Bovolo, L. Bruzzone, and S. Marchesi, "Analysis and adaptive estimation of the registration noise distribution in multitemporal VHR images," *IEEE Trans. Geosci. Remote Sens.*, vol. 47, no. 8, pp. 2658–2671, 2009.

[9] S. Marchesi, F. Bovolo, and L. Bruzzone, "A context-sensitive technique robust to registration noise for change detection in VHR multispectral images," *IEEE Trans. Geosci. Remote Sens.*, vol. 19, no. 7, pp. 1877–1889, Jul. 2010.

[10] J. C. Chan, K. Chan, and A. G. Yeh, "Detecting the nature of change in an urban environment: A comparison of machine learning algorithms," *Photogramm. Eng. Remote Sens.*, vol. 67, no. 2, pp. 213–225, Feb. 2001.

[11] D. Fernandez-Prieto and M. Marconcini, "A novel partially supervised approach to target change detection," *IEEE Trans. Geosci. Remote Sens.*, vol. 49, no. 12, pp. 5016–5038, Dec. 2011.

[12] X. Huang and L. Zhang, "A multidirectional and multiscale morphological index for automatic building extraction from multispectral GeoEye-1 imagery," *Photogramm. Eng. Remote Sens.*, vol. 77, no. 7, pp. 721–732, Jul. 2011.

[13] X. Huang and L. Zhang, "Morphological building/shadow index for building extraction from high-resolution imagery over urban area," *IEEE J. Sel. Topics Appl. Earth Observ. Remote Sens.*, vol. 5, no. 1, pp. 161–172, Feb. 2012.

[14] C. Harris and M. Stephens, "A combined corner and edge detector," in *Proc. AVC*, 1988, pp. 147–151.

[15] Z. Xiong and Y. Zhang, "A novel interest-point matching algorithm for high-resolution satellite images," *IEEE Trans. Geosci. Remote Sens.*, vol. 47, no. 12, pp. 4189–4200, Dec. 2009.